Available online at www.sciencedirect.com
SciVerse ScienceDirect
Ceramics International 39 (2013) 3065–3075
CERAMICS INTERNATIONAL
www.elsevier.com/locate/ceramint

Optimization of the production process through response surface method: Bricks made of loess

Milica Arsenović[a,*], Slavka Stanković[b], Lato Pezo[c], Lidija Mančić[d], Zagorka Radojević[a]

[a]Institute for Testing of Materials IMS, Bulevar vojvode Mišića 43, 11000 Belgrade, Serbia
[b]University of Belgrade, Faculty of Technology and Metallurgy, Karnegijeva 4, 11000 Belgrade, Serbia
[c]University of Belgrade, Institute of General and Physical Chemistry, Studentski trg 12, 11000 Belgrade, Serbia
[d]Institute of Tecnical Sciences of SASA, Knez Mihailova 35, 11000 Belgrade, Serbia

Received 18 September 2012; received in revised form 25 September 2012; accepted 25 September 2012
Available online 2 October 2012

Abstract

Loess clays are commonly used to produce bricks. Heavy clays, taken at location near Zrenjanin, Serbia, are used as a representative raw material in this study. The sample, containing about 28% of clay sized particles, is enriched using two more plastic heavy clays from neighboring locations. Chemical and mineralogical content of clays is determined, as well as particle size distribution. Optimization of the processing parameters during the bricks production, i. e. temperature (900–1100 °C), and concentration of 2 clays combined addition (both in the range of 0–10%), is done based on the following independent parameters: compressive strength (*CS*), water absorption (*WA*), firing shrinkage (*FS*), weight loss during firing (*WLF*) and apparent density expressed as volume mass of cubes (*VMC*). Developed models showed r^2 values in the range of 0.822–0.998, and they were able to accurately predict *CS*, *WA*, *FS*, *WLF* and *VMC* in a wide range of processing parameters. The optimum conditions are determined by the response surface method (RSM), coupled with the fuzzy synthetic evaluation (FSE) algorithm, using membership trapezoidal function, with defined optimal interval values, depending on a final usage of the raw material in heavy clay brick industry.

Keywords: Heavy clay brick; Loess deposits; Response surface method

1. Introduction

Ceramic and technological properties of heavy clay ceramic products depend on feeding material characteristics such as: mineralogy [1], chemistry [2], particle size distribution [3] and plasticity [4], but also on firing conditions determined by the temperature, heating rate and kiln atmosphere [5–7]. Mathematical tools for assessing the impact of raw material properties and processing parameters on the quality of the final product are used intensively used in this field from recently [8–12].

The response surface methodology (RSM) has been proven as useful method for determining the influence of process variables on a group of dependent parameters that are significant for the process and effects studied [11–13]. RSM is an effective tool for optimizing a variety of processes, especially in design of mixture experiments [11]. The RSM equations describe effects of the test variables on the observed responses, determine test variables interrelationships and represent the combined effect of all test variables in the observed responses, enabling the efficient investigation of the process [12]. The main advantage of RSM is reduced number of experimental runs that provide sufficient information for statistically valid results, along with determination of a response value for any chosen natural variable belonging to the investigated experimental domains. RSM is also proven to be an effective tool for optimizing ceramic materials [11,12].

Serbian brick industry dominantly uses loess raw materials. The most abundant component of these heavy clays is silt (up 80 wt%). Mineralogical composition includes clay minerals, quartz and carbonates, which can be either finely dispersed or in the form of loess concretions, called. “loess dolls”, which are tied to particular layers of loess (usually lower ones). Loess

*Corresponding author. Tel.: +381 112650650.
E-mail address: milica.arsenovic@institutims.rs (M. Arsenović).

0272-8842/$ - see front matter
http://dx.doi.org/10.1016/j.ceramint.2012.09.086

Table 1
Chemical and mineralogical composition of the used raw materials.

Chemical composition in wt%											
	SiO_2	Al_2O_3	Fe_2O_3	CaO	MgO	Na_2O	K_2O	MnO	TiO_2	SO_3	L.O.I.
RRM	53.93 ± 0.78^{a}	12.66 ± 0.11^{a}	5.34 ± 0.07^{ab}	6.67 ± 0.05^{c}	2.83 ± 0.02^{a}	1.25 ± 0.01^{c}	3.00 ± 0.03^{c}	0.07 ± 0.00^{b}	1.33 ± 0.00^{c}	0.17 ± 0.00^{b}	12.75 ± 0.07^{c}
HC1	57.36 ± 0.53^{b}	16.08 ± 0.17^{b}	5.46 ± 0.03^{b}	5.51 ± 0.06^{a}	2.88 ± 0.02^{b}	1.08 ± 0.01^{b}	2.20 ± 0.01^{b}	0.07 ± 0.00^{a}	0.29 ± 0.00^{b}	0.01 ± 0.00^{a}	9.07 ± 0.05^{b}
HC2	56.09 ± 0.32^{b}	17.65 ± 0.12^{c}	5.29 ± 0.04^{a}	5.79 ± 0.03^{b}	3.00 ± 0.02^{c}	1.04 ± 0.01^{a}	1.89 ± 0.01^{a}	0.08 ± 0.00^{c}	0.27 ± 0.00^{a}	0.01 ± 0.00^{a}	8.90 ± 0.07^{a}
Mineral composition and particle size distribution in wt%											
	Q	I	Ch.	Sm.	K	C	D	F	< 2 μm	2–20 μm	> 20 μm
RRM	++	+	+	+	–	+	+	+	28.55	59.45	12.00
HC1	++	+	+	+	–	+	+	+	42.65	44.85	12.50
HC2	++	+	+	+	–	+	+	+	40.65	49.40	9.95

Q – quartz, I – illite, Ch. – chlorite, Sm. – smectite, K – kaolinite, C – calcite, D – dolomite, F – feldspar.
++ present in high quantity, + present in low quantity, – not present.
[a,b,c]Values with the same letter, written in superscript are not statistically different at the $p<0.05$ level, 95% confidence limit, according to post-hoc Tukey's HSD test.

contains a considerable amount of carbonates (calcite, and to a lesser extent dolomite), even up to 35 wt%. If carbonates are finely dispersed and uniformly distributed, they react in the firing process with clay minerals, chlorite and mica, forming calcium silicates, which improves mechanical properties. Calcite present in loess significantly reduces firing shrinkage and decreases density, by increasing porosity and water absorption of final products. The presence of carbonates in loess in the form of larger concretions and "loess dolls" is common. Large calcite particles remain in the form of CaO after firing. Due to the hydration of CaO and generation of $Ca(OH)_2$, an increase in volume occurs. By binding of CO_2 from the air, $Ca(OH)_2$ turns to carbonate, increasing further product volume for about three times of the CaO initial volume. This can often cause the emergence of "popping" of the product and even its damage. However, favorable particle size distribution, low shrinkage and sensitivity to drying and firing ease the production. This is especially true in the case of small plants at a low level of technology and equipment. Such raw material is not suitable for the application, or it requires special processing line with a cleaner machine, and grinding in degrees to grade below 0.5 mm [14,15].

Loess is an eolian sedimentary deposit that consists of various clay and silt sized minerals. Loess and loess-like sediments cover as much as 10 wt% of Earth's surface, and form some of the world's most productive soils. In terms of morphology, terrain in Zrenjanin, Serbia consists of loess terraces, loess plateaus, and also fossil fluvial landforms—alluvial plains and river terraces. Largest area on the surface of the region is occupied by quaternary sediments, represented by equivalents of older and younger Pleistocene and Holocene, which consist of sand, gravel, alevrites and clay within river and swamp sediments. Loess can represent extremely sandy to high plastic material, but deposits quality mostly varies. Alternation of silty loess layers and clay, with inserted fluvial sequences shows that the origin of the material is combination of eolian and fluvial brought by waterways. Changes in deposited loess during interglacial warmer intervals of the ice age lead to decarbonization, when clayey layers occur, which are called buried soil (or fossil soil). Buried soil contains different clay minerals which improve raw material plasticity. In all types of deposits unwanted components can be found, such as $CaCO_3$ present in the form of concretions. Some layers can contain calcite to a quantity that make up raw material unusable without proper pre-treatment, while in some deposits it may occur in the form of veins or tiles, with a devastating effect on the product [14,16,17].

Brick factories whose mines contain several layers of buried soil produce hollow products (clay blocks). Swamp loess can be used in the manufacture of hollow clay bricks and roof tiles, because of the increased content of clay minerals. Hollow clay products made of loess have thick walls, high volume mass and therefore require more energy upon thermal treatment [14].

In this study representative heavy clay raw material was chosen and is combined further with two higher plastic clays added in different content (both are varied between 0–10 wt%), all sampled near Zrenjanin, Serbia. Second order polynomial models for determination of 10 response variables are developed, and correlation coefficients among them are determined afterward. PCA showed grouping of designed samples by the firing temperature and response variables. Determination of the optimum processing conditions is done by using the response surface method, coupled with the fuzzy synthetic evaluation (FSE) algorithm through using membership trapezoidal function, with defined optimal interval values determined by the final usage of the raw material in heavy clay brick industry. Process variables were firing temperature and concentrations of added heavy clays.

2. Materials and methods

The representative raw material (RRM) and two more plastic heavy clays (heavy clay 1—HC1 and heavy clay 2—HC2) were collected in Zrenjanin, Serbia, and belong to loess clays.

2.1. Chemical and mineralogical composition

Major oxides chemical content is determined using classical silicate analysis [9], while all the measurements are performed in triplicate.

The mineralogical analysis is carried out by X-ray diffraction (XRD) using a powder diffractometer (Philips PW-1050), with λCu–Kα radiation and scanning speed of 0.05 °C/s, both on powder (bulk samples) and oriented aggregates (treated with ethylene glycol and heated to 450 °C for 2 h) of the clay fraction obtained, according to the existing criteria [18]. A semi-quantitative analysis is carried out following the literature methodology [19].

Particle size distribution (PSD) was determined by granulometry analysis done by the pipette method, after drying of samples at room temperature. The sample was dipped in distilled water for 24 h, and then gently boiled for 1 h. Cooled suspension was sieved on the 0.063 mm sieve, the fraction is dried and measured, and later the filtrate was treated in an ultrasonic bath for 30 min. Samples are taken by the pipette at appropriate intervals. Due to the size of particles, it was necessary to perform sedimentation analysis (fractions under 0.063 mm).

2.2. Technological characteristics after firing

After collecting, the samples are oven-dried at 105 °C until constant mass, and then milled following the normal practice in ceramic laboratories. To simulate industrial pressing conditions, RRM, HC1 and HC2, and appropriate mixes (see Tables 2 and 3.) are moistened by hand, mixed sufficiently and milled to 2 mm until homogeneous mass with about 21–24 wt% of water were obtained. The samples are left to rest for 24 h in sealed nylon bags, in order to homogenize the moist. The shaping process is done in the usual procedure [20] using laboratory extruder (*Händle*). Laboratory samples are produced in the form of tiles (120 × 50 × 14 mm^3), hollow blocks with vertical voids (55.3 × 36 × 36 mm^3) and cubes (30 × 30 × 30 mm^3). After shaping, the samples are dried in the air, and later in a laboratory dryer at 105 ± 5 °C to a constant mass. Firing is done in the electrical furnace with oxygen atmosphere, at average heating speed of 1.4 °C/min until 610 °C, and further at the rate of 2.5 °C/min up to the final designated temperature, at which the samples were treated for 2 h [9]. Firing of all groups of samples is conducted at 900 °C, 950 °C and 1000 °C.

Table 2
Coded values of the process variables.

	Treatment variables	Coded values		
		−1	0	+1
X_1	Temperature (°C)	900	1000	1100
X_2	[HC1] (%)	0	5	10
X_3	[HC2] (%)	0	5	10

Compressive strength (*CS*) is determined in a laboratory hydraulic press Alfred Amsler, CHD, with measuring range of 100/200/500/1,000 kN and resolution of 0.1/0.2/0.5/1 kN. Three specimens for each combination of sample shape (blocks and cubes) and firing temperature are tested. The samples are flattened to ensure that the surfaces are parallel. *CS* is then tested on single samples (without mortar usage), with bottom area of 0.002 m^2 for blocks and 0.0009 m^2 for cubes, and a loading rate of 0.6 kN/s. The strength results reported represent the average values of three specimens, with a variation of no more than 10%.

Water absorption (*WA*) is evaluated by soaking samples in water for 24 h, according to standard SRPS EN 771-1 [21], and later volume mass of cubes (*VMC*), which represented apparent density, is calculated as weight of fired samples divided by the volume of water displaced by flooding in the measuring cilinder [22]. Weight loss during firing (*WLF*) is determined by measuring on a scale with 0.001 g precision, and calculated as a quotient between the mass loss during firing and a starting weight of sample, and later expressed in %. Firing shrinkage (*FS*) was obtained by the relative variation in length of the tiles using a caliper (precision of ± 0.01 mm).

2.3. Statistical analysis

The RSM method was selected to estimate the main effect of the process variables on *CS*, *WA*, *FS*, *WLF* and *VMC*. The accepted experimental design was taken from Box and Behnken [23]. The independent variables were: firing temperature (X_1) of 900 °C, 1000 °C and 1100 °C; concentrations of HC1 (X_2) and HC2 (X_3) of 0, 5 and 10 wt% ([HC1] and [HC2]). The dependent variables observed were the responses: compressive strength of

Table 3
Experimental design and data for the response surface analysis.

Run no.	Process parameters			Responses									
	X_1 temp. (°C)	X_2 [HC1] (%)	X_3 [HC2] (%)	Y_1 *CSB* (MPa)	Y_2 *CSC* (MPa)	Y_3 *WAT* (%)	Y_4 *WAB* (%)	Y_5 *WAC* (%)	Y_6 *FS* (%)	Y_7 *WLFT* (%)	Y_8 *WLFB* (%)	Y_9 *WLFC* (%)	Y_{10} *VMC* (%)
1	−1	−1	−1	26.75	36.24	18.33	17.28	12.70	0.94	9.64	9.91	10.39	1.74
2	−1	−1	0	26.32	37.62	18.60	17.60	13.05	1.09	9.60	9.90	10.36	1.75
3	−1	−1	1	25.96	38.97	18.84	17.91	13.37	1.22	9.55	9.88	10.32	1.75
4	−1	0	−1	26.38	37.38	18.52	17.53	12.96	0.94	9.55	9.86	10.34	1.74
5	−1	0	0	26.01	38.76	18.77	17.84	13.28	1.08	9.51	9.84	10.30	1.75
6	−1	0	1	25.70	40.11	19.00	18.12	13.58	1.19	9.47	9.82	10.26	1.75
7	−1	1	−1	26.06	38.54	18.70	17.76	13.20	0.94	9.47	9.81	10.28	1.75
8	−1	1	0	25.74	39.91	18.93	18.05	13.50	1.06	9.42	9.79	10.25	1.75
9	−1	1	1	25.49	41.26	19.14	18.31	13.78	1.16	9.38	9.77	10.21	1.75
10	0	−1	−1	30.40	38.18	18.02	16.96	11.66	0.60	9.84	10.24	10.74	1.75
11	0	−1	0	30.02	39.96	18.28	17.27	11.98	0.78	9.79	10.22	10.71	1.76
12	0	−1	1	29.71	41.72	18.52	17.56	12.28	0.94	9.75	10.20	10.67	1.76
13	0	0	−1	30.05	39.68	18.20	17.19	11.90	0.65	9.75	10.19	10.68	1.75
14	0	0	0	29.72	41.46	18.45	17.49	12.20	0.82	9.70	10.16	10.65	1.76
15	0	0	1	29.46	43.21	18.67	17.75	12.48	0.96	9.65	10.13	10.61	1.76
16	0	1	−1	29.74	41.19	18.38	17.41	12.12	0.68	9.65	10.13	10.62	1.75
17	0	1	0	29.47	42.96	18.60	17.69	12.40	0.84	9.61	10.10	10.58	1.76
18	0	1	1	29.26	44.71	18.81	17.94	12.66	0.97	9.56	10.07	10.54	1.76
19	1	−1	−1	38.46	54.13	16.91	16.23	9.81	0.56	9.92	10.37	10.89	1.78
20	1	−1	0	38.13	56.31	17.16	16.53	10.12	0.78	9.87	10.35	10.86	1.78
21	1	−1	1	37.86	58.47	17.39	16.81	10.39	0.97	9.82	10.31	10.81	1.78
22	1	0	−1	38.12	55.97	17.09	16.46	10.04	0.65	9.82	10.31	10.83	1.78
23	1	0	0	37.84	58.16	17.32	16.74	10.32	0.85	9.77	10.28	10.79	1.78
24	1	0	1	37.62	60.31	17.54	16.99	10.57	1.03	9.72	10.24	10.75	1.78
25	1	1	−1	37.82	57.83	17.25	16.67	10.24	0.73	9.72	10.24	10.77	1.78
26	1	1	0	37.59	60.01	17.47	16.92	10.50	0.91	9.67	10.21	10.72	1.78
27	1	1	1	37.43	62.17	17.67	17.16	10.73	1.07	9.63	10.18	10.68	1.78

blocks–*CSB* (Y_1) and cubes–*CSC* (Y_2); water absorption of tiles–*WAT* (Y_3), blocks–*WAB* (Y_4) and cubes–*WAC* (Y_5); firing shrinkage–*FS* (Y_6); weight loss during firing of tiles–*WLFT* (Y_7), blocks–*WLFB* (Y_8) and cubes–*WLFC* (Y_9); and apparent density expressed as volume mass of cubes–*VMC* (Y_{10}).

The experimental data used for the optimization study were obtained using central composite full factorial design (3 level-3 parameter) with 27 runs (1 block) [23]. A model was fitted to the response surface generated by the experiment. The model used was function of the process variables

$$Y_k = f_k(\text{temperature}, \text{HC1}, \text{HC2}) \quad (1)$$

Ten second order polynomial (SOP) models of the following form were developed to relate ten responses (Y) such as: *CSB*, *CSC*, *WAT*, *WAB*, *WAC*, *FS*, *WLFT*, *WLFB*, *WLFC* and *VMC* to three process variables (X), i.e. temperature, concentration of HC1 and HC2:

$$Y_k = \beta_{k0} + \sum_{i=1}^{3} \beta_{ki} X_i + \sum_{i=1}^{3} \beta_{kii} X_i^2 + \sum_{i=1}^{2} \sum_{j=i+1}^{3} \beta_{kij} X_i X_j \quad (2)$$

where: β_{kn} were constant regression coefficients. The significant terms and the validity of the models were found using ANOVA for each response.

Analysis of variance (ANOVA) and RSM were performed using the StatSoft Statistica, *v*.10 for Windows. The model was obtained for each dependent variable (or response), where factors were rejected when their significance level was less than $p < 0.05$, confidence limit 95%. The same program was used for generation of graphs and contour plots.

Principal component analysis (PCA) was utilized to analyze variable independency, as a well-known mathematical procedure used as exploratory data analysis, enabling a differentiation between the samples [9].

The Fuzzy synthetic optimization method was implemented using the results of models proposed, to represent *CSB*, *CSC*, *WAT*, *WAB*, *WAC*, *FS*, *WLFT*, *WLFB*, *WLFC* and *VMC*, according to Eq. (2). FSE is commonly used technique to solve problems with constraints involving non-linear functions. These methods aim to solve a sequence of simple problems whose solutions converge to the solution of the original problem [10].

Trapezoidal membership function used, could be written as

$$A(x,\ a,\ m,\ n,\ b) = \begin{cases} a \le x < m, & \dfrac{x-a}{m-a} \\ m \le x < n, & 1 \\ n \le x < b, & 1-\dfrac{x-n}{b-n} \end{cases} \quad (3)$$

where x is either *CSB*, *CSC*, *WAT*, *WAB*, *WAC*, *FS*, *WLFT*, *WLFB*, *WLFC* or *VMC*, and the values of a, b, m and n are function parameters. Interval a—b represent the range in which measured values occur, while range m—n is the expected optimal values range for response variables, chosen for certain products groups.

An optimization with procedure was performed according to FSE algorithm, using the MicroSoft Excel 2007 to determine the workable optimum conditions for the thermal processing of heavy clay bricks. After the optimum conditions were established, separate experiments are performed in order to validate the models.

3. Results and discussion

3.1. Chemical and mineralogical composition

The chemical and mineralogical compositions of the used materials, together with particle size distribution, are given in Table 1, where L.O.I. represents loss on ignition values while heating from 105 to 1000 °C. Post ANOVA's Tukey HSD (honestly significant difference) test, at the $p < 0.05$ significant level (95% confidence limit) was performed in order to access the statistically significant differences within each chemical composition assay. Descriptive statistical analyses, for calculating the means and the standard error of the mean, were performed using the Microsoft Excel 2007 software. All obtained results were expressed as the mean ± standard deviation (SD).

Statistically significant differences were observed in most chemical composition assays, as shown in Table 1. Tukey's test showed that the similar SiO_2 content was found in HC1 and HC2 samples. According to SiO_2 and Al_2O_3 content, it is obvious that the highest clay content contained sample HC1, and the lowest sample RRM. Quotient between the molar fractions of SiO_2 and Al_2O_3 implies the existence of free SiO_2, here present in the form of quartz [24]. PSD analysis results confirmed that the highest quartz content was found in the sample HC1, and the lowest in the sample HC2. All the samples contain similar carbonates composition, while RRM showed the highest calcite, and HC2 the highest dolomite content.

Mineralogical analysis revealed that all the samples contained mostly of quartz, illite, chlorite, smectite, calcite, dolomite and feldspar (plagioclase). Variations of fine silt (20–2 μm) and clay (< 2 μm) fractions illustrated the intensity of sediments weathering process. Silt content increased from older to younger layers. In contrast, the clay fraction record showed decreasing trend in clay from older to younger fossil soils [15]. Sample HC1 was taken from the lowest layer and represents the oldest one, while RRM was the youngest and the closest to the surface. The highest illite content was observed in the sample RRM, which was proven by the highest K_2O and Na_2O content [25]. The oldest layers (HC1 and HC2) developed so called "forest soil" (clay sized particles content ranging from 31 to 46 wt%), indicating warm and humid paleoclimatic conditions [15].

3.2. Ceramic and technological features after firing

Variation of temperature and concentrations of HC1 and HC2 were coded according to Table 2.

Table 4
Correlation coefficients, with statistical significance expressed as *p*-level values, written in parentheses.

	CSC	*WAT*	*WAB*	*WAC*	*FS*	*WLFT*	*WLFB*	*WLFC*	*VMC*
CSB	0.94^{*} (<0.01)	-0.95^{*} (<0.01)	-0.88^{*} (<0.01)	-0.98^{*} (<0.01)	-0.47^{*} (0.01)	0.75^{*} (<0.01)	0.87^{*} (<0.01)	0.88^{*} (<0.01)	0.98^{*} (<0.01)
CSC		-0.84^{*} (<0.01)	-0.70^{*} (<0.01)	-0.87^{*} (<0.01)	-0.18^{ns} (0.36)	0.50^{*} (0.01)	0.69^{*} (<0.01)	0.70^{*} (<0.01)	0.98^{*} (<0.01)
WAT			0.98^{*} (<0.01)	0.98^{*} (<0.01)	0.58^{*} (<0.01)	-0.81^{*} (<0.01)	-0.84^{*} (<0.01)	-0.86^{*} (<0.01)	-0.89^{*} (<0.01)
WAB				0.95^{*} (<0.01)	0.71^{*} (<0.01)	-0.89^{*} (<0.01)	-0.85^{*} (<0.01)	-0.87^{*} (<0.01)	-0.79^{*} (<0.01)
WAC					0.59^{*} (<0.01)	-0.83^{*} (<0.01)	-0.91^{*} (<0.01)	-0.92^{*} (<0.01)	-0.93^{*} (<0.01) *
FS						-0.75^{*} (<0.01)	-0.70^{*} (<0.01)	-0.72^{*} (<0.01)	-0.30^{ns} (0.12)
WLFT							0.93^{*} (<0.01)	0.93^{*} (<0.01)	0.63^{*} (<0.01)
WLFB								0.99^{*} (<0.01)	0.78^{*} (<0.01)
WLFC									0.79^{*} (<0.01)

^{ns}Not significant.
*Significant at 95% confidence level.

The experimental data used for the optimization study were obtained using central composite full factorial design (3 level-3 parameter) with 27 runs (1 block), as shown in Table 3. When adding solely HC1 or HC2, or with changing one of HCs while preserving the other HC content constant, most of the response variables increase (*CSC*, *WA* and *FS*), while *CSB* and *WLFT* decrease, and *VMC* remains almost the same. Higher clay minerals content causes better particles packing, as well as ability of the materials to sinter. *CSC* is higher also because of carbonates react with clay minerals, giving calcium and magnesium silicates. The drop of *CSB* with HC1 or HC2 addition may be caused by weaker grain diffusion in hollow blocks. The rest of unreacted carbonates are burned out leaving the pores behind and increasing open porosity so *WA* rise [10,12,26]. HC1 addition inserts greater changes in the behavior of laboratory samples then HC2, while tiles and cubes response values differ less. Actually, HC1 contains more clay sized particles, less carbonates and less silt (alevrolite) fraction, so its addition leads to the improvement of ceramic and technological behavior. With addition of HC1 and/or HC2, higher firing temperature caused increase of *CS*, *WLF FS* and *VMC* values and decrease of *WA*.

3.3. Correlation analysis of responses

Response variables were tested for independency, using correlation analysis, Table 4. It was found that *CS* and *WA* variables correspond very well to each other, with high significance level $p<0.01$, at 95% confidence limit. Correlation between *CS* and *WA* groups of variables gained negative sign in analysis, which means that an increase in *CS* has decreased *WA*. *CS* group of variables correlated with *VMC* with correlation coefficient of 0.98.

The correlations between the groups of variables were very high: for *CSC* and *CSB* it was 0.94, for *WAT*, *WAB* and *WAC* between 0.95 and 0.98, and for *WLFT*, *WLFB* and *WLFC* between 0.93 and 0.99.

3.4. Principal component analysis (PCA) of responses

Mechanical measurment results showed that the first two principal components, accounting for 94.96% of the total variability can be considered sufficient for data representation (Fig. 1). PCA showed the grouping of *CSB* and *CSC*; *WAB*, *WAC* and *WAT*; and also *WLFT*, *WLFB* and *WLFC*, as expected, and as it was shown in correlation analysis. Negative correlation between *CS* and *WA* groups of responces is also confirmed. Furthermore, *VMC* correlated good with *CSB* and *CSC*, while *FS* negatively correlated with *WLF* group of variables. PCA clearly discriminated heavy clay samples into three groups according to firing temperature: 900 °C (samples 1–9), 1000 °C (samples 10–18) and 1100 °C (samples 19–27), which could lead to conclusion that the temperature is the main influential processing parameter. This confirms our previous studies results [9,10].

Both correlation analysis and PCA showed that some response variables were not independant, but all proposed variables (*CSB*, *CSC*, *WAT*, *WAB*, *WAC*, *FS*, *WLFT*, *WLFB*, *WLFC* and *VMC*) were used for further statistical analysis, according to common practice.

3.5. ANOVA and RSM analysis

In this study, ANOVA was conducted to show the significant effects of the independent variables to the responses and which of responses were significantly affected by the varying treatment combinations. Table 5 shows the ANOVA calculation regarding the response models developed when the experimental data were fitted to a response surface. The effect of each variable is quantified by its sum of squares (SS). The response surface used a (SOP) in the form of Eq. (2) in order to predict the function f_k (Eq. (1)) for all the dependent variables.

The analysis revealed that the linear terms contributed substantially in the majority of cases to generate a significant SOP models. The SOP models for all variables were found to be statistically significant and the response surfaces were fitted to these models. The linear terms of temperature were found significant at $p<0.05$ level, 95% confidence level, and its influence were found most important for *CSB*, *CSC*, *WAT*, *WAB*, *WAC*, *FS*, *WLFT*, *WLFB*, and *WLFC* calculation. This conclusion confirmed grouping of samples in PCA. The influence of quadratic term of temperature is also very important for *CSB* and *CSC* calculation, also significant at $p<0.05$ level and 95% confidence level. Most probably is that the temperature affects more samples containing more carbonates, so with increase of their presence quadratic term of temperature can become more influential then linear [10]. Non-linear terms in SOP model for *WAB* and *WAC* calculation were found insignificant. For FS calculation, linear term of temperature in SOP model is the most influential, while other linear and quadratic terms were found statistically insignificant, or with minor influence. All linear terms for *WLFT*, *WLFB*, and *WLFC* calculation were found statistically significant, while non-linear terms were found to be of minor influence or statistically insignificant. Thus, it is concluded that most of the responses were influenced by separate process parameters, and not by their combined affect. The only exception was *VMC*, most affected by non-linear term Temp × [HC1], and linear term of temperature was found statistically insignificant.

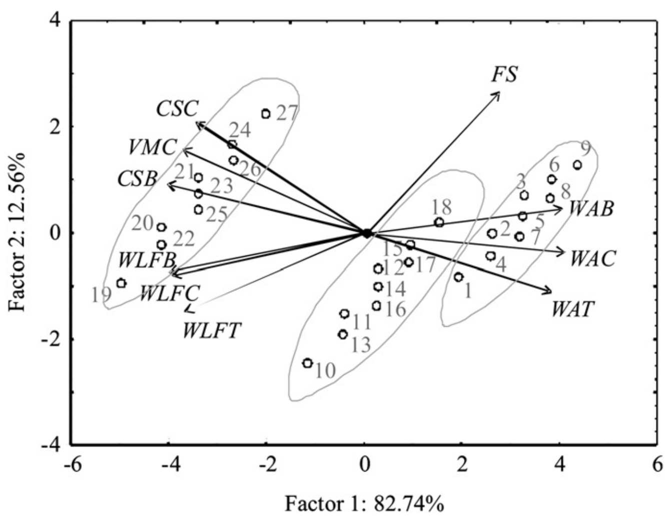

Fig. 1. Biplot for mechanical characteristics of heavy clay samples.

The residual variance also shown in Table 4, where the error term represent the lack of fit variation, i.e., it represents other contributions except the linear, quadratic and cross product terms. All SOP models had insignificant lack of fit tests, which means that all the models represented the data satisfactorily.

A high r^2 indicates that the variation was accounted and that the data fitted satisfactorily to the proposed SOP models. The r^2 values for *CSB* (99.61), *CSC* (99.76), *WAT* (99.74), *WAB* (92.08), *WAC* (99.61), *FS* (99.81), *WLFT* (99.27),

Table 5
Analysis of variance for the eight responses, 3 factors, 1 block and 27 runs.

Term	Source	*dF*	*CSB*	*CSC*	*WAT*	*WAB*	*WAC*	*FS*	*WLFT*	*WLFB*	*WLFC*	*VMC*
Linear	Temp	1	413.34*	1674.52*	90.07*	0.28*	34.23*	0.43*	9.48*	51.28*	50.36*	0.00^{ns}
	[HC1]	1	2.10*	13.19*	0.25*	2.11*	1.36*	0.00*	0.96*	0.07*	0.17*	0.00*
	[HC2]	1	0.01^{ns}	13.87*	0.79*	0.33*	1.28*	0.02*	0.27*	0.07*	0.02**	0.00*
Quad.	Temp	1	213.83*	91.09*	0.01^{ns}	0.19*	0.53*	0.01*	0.00^{ns}	0.02**	0.00^{ns}	0.00^{ns}
	[HC1]	1	0.31^{ns}	0.93**	0.03^{ns}	0.13*	0.01^{ns}	0.00**	0.04*	0.00^{ns}	0.01^{ns}	0.00*
	[HC2]	1	1.77*	0.05^{ns}	0.00^{ns}	0.0^{ns}	0.17*	0.00^{ns}	0.39*	0.00^{ns}	0.03*	0.00*
Product	Temp × [HC1]	1	0.54**	1.69*	0.13*	0.96*	0.19*	0.00*	0.01^{ns}	0.00^{ns}	0.01^{ns}	0.01*
	Temp × [HC2]	1	2.73*	2.10*	0.05^{ns}	0.83*	0.10*	0.00*	0.03*	0.00^{ns}	0.06*	0.00*
	[HC1] × [HC2]	1	23.69*	0.19^{ns}	0.01^{ns}	0.01*	0.03*	0.00^{ns}	0.16*	0.00^{ns}	0.00^{ns}	0.00*
Error	Error	17	2.58^{ns}	4.31^{ns}	0.24^{ns}	0.42^{ns}	0.15^{ns}	0.00^{ns}	0.08^{ns}	0.08^{ns}	0.08^{ns}	0.00^{ns}
r^2			99.61	99.76	99.74	92.08	99.61	99.81	99.27	99.85	99.85	92.57

dF-degrees of freedom.
^{ns}Not significant.
*Significant at 95% confidence level.
**Significant at 90% confidence level.

Table 6
Regression coefficients (based on coded data) of the SOP models for the ten responses.

	CSB	*CSC*	*WAT*	*WAB*	*WAC*	*FS*	*WLFT*	*WLFB*	*WLFC*	*VMC*
β_0	580.98 ± 15.91	343.47 ± 20.56	-8.23 ± 3.81	-4.52 ± 1.81	-3.44 ± 0.81	4.22 ± 0.29	17.80 ± 2.85	-10.30 ± 2.79	-4.35 ± 2.11	1.44 ± 0.43
β_1	-1.15 ± 0.03	-0.69 ± 0.04	0.03 ± 0.01	0.04 ± 0.01	0.05 ± 0.01	-0.01 ± 0.00	0.02 ± 0.01	0.03 ± 0.01	0.02 ± 0.01	0.01 ± 0.001
β_{11}	0.00 ± 0.00	0.00 ± 0.00	–	0.00 ± 0.00	0.00 ± 0.00	0.00 ± 0.00	–	–	–	–
β_2	–	-0.71 ± 0.30	0.21 ± 0.07	0.57 ± 0.09	0.31 ± 0.06	-0.02 ± 0.00	-0.10 ± 0.04	–	–	-0.06 ± 0.01
β_{22}	–	–	–	0.01 ± 0.00	–	–	0.00 ± 0.00	–	–	0.00 ± 0.00
β_3	-0.90 ± 0.24	–	–	0.53 ± 0.09	-0.21 ± 0.06	–	–	–	-0.17 ± 0.04	0.04 ± 0.01
β_{33}	0.02 ± 0.01	–	–	–	0.01 ± 0.00	–	-0.01 ± 0.00	–	0.00 ± 0.00	0.00 ± 0.00
β_{12}	–	0.00 ± 0.00	0.00 ± 0.00	0.00 ± 0.00	0.00 ± 0.00	0.00 ± 0.00	–	–	–	0.00 ± 0.00
β_{13}	0.00 ± 0.00	0.00 ± 0.00	–	0.00 ± 0.00	0.00 ± 0.00	0.00 ± 0.00	0.00 ± 0.00	–	0.00 ± 0.00	0.00 ± 0.00
β_{23}	-0.06 ± 0.00	–	–	–	–	–	0.00 ± 0.00	–	–	0.00 ± 0.00

WLFB (99.85), *WLFC* (99.85) and *VMC* (92.57) confirmed the good fitting of the model to the experimental results.

Table 6 shows the regression coefficients for the response SOP models of *CSB*, *CSC*, *WAT*, *WAB*, *WAC*, *FS*, *WLFT*, *WLFB*, *WLFC* and *VMC*, used by Eq. (2) for predicting the values at optimum conditions. The analysis revealed that the linear, quadratic and interchange terms contributed substantially in all cases to generate a significant SOP model. The SOP models for all variables were found to be statistically significant and the fitting of experimental data was good.

Water absorption, along with open porosity and linear shrinkage, are physical parameters that can be used for optimizing the production of materials [27]. After thermal production of bricks it is essential to gain optimal values of *CSB*, *CSC*, *WAT*, *WAB*, *WAC*, *FS*, *WLFT*, *WLFB*, *WLFC* and *VMC*, depending on the final product application. It is not necessary, for example, to spend a lot of energy and get an extra hard product. It is enough to find the optimal firing temperature which would contribute to satisfying properties of a certain sort of a product. The choice of the best process conditions (firing temperature, concentration of added heavy clays) for production of bricks depends on the application that would be given to the product.

Multiple fuzzy synthetic optimization of the ten response variables was accomplished in order to find the processing variables (firing temperature, concentrations of HC1 and HC2), that give optimal values of *CSB*, *CSC*, *WAT*, *WAB*, *WAC*, *FS*, *WLFT*, *WLFB*, *WLFC* and *VMC*. Trapezoidal membership function was used as optimization method, according to Eq. (3), in which *a—b* covered the complete interval where obtained values for separately tested RRM, HC1 and HC2 fired samples were found [10], and *m—n* represented the optimal values for observed product group (Table 7). The optimum ranges were given based on our experience with heavy clay, knowing that each ceramic product requires clays having particular and appropriate characteristics [4].

Heavy clay products were divided into three groups

1. Group I is suitable for the production of solid bricks, due to the low clay and high carbonates content, which causes low plasticity. In order to improve the product quality, more plastic clay should be added in the mixture for hollow blocks shaping.
2. Group II can be used for producing hollow bricks and blocks, as well as ceiling elements.
3. Group III can be, after grinding below 0.5 mm to avoid the appearance of lime corns, used in roof tiles and facade elements production. The samples belonging to Groups II and III can be also used in a light-weighted bricks, as a primary raw material [10].

The objective function (*F*) is the mathematical function whose maximum would be determined, by summing the FSE results for of the five models, according Eq. (1). All groups of response variables (*CS*, *WA*, *WLF*, *FS* and *VMC*) have

Table 7
Optimal ranges of responses, for different groups of products.

Group	Param.	*CSB*	*CSC*	*WAT*	*WAB*	*WAC*	*FS*	*WLFT*	*WLFB*	*WLFC*	*VMC*
–	*a*	25.49	36.24	16.91	16.23	9.81	0.56	9.38	9.77	10.21	1.74
	b	38.46	62.17	19.14	18.31	13.78	1.22	9.92	10.37	10.89	1.78
I	*m*	13.00	25.00	21.00	21.00	21.00	−0.54	10.20	10.20	10.20	1.62
	n	17.00	35.00	25.00	25.00	25.00	0.11	14.30	14.30	14.30	1.81
II	*m*	24.00	45.00	16.00	16.00	16.00	0.34	8.20	8.20	8.20	1.76
	n	28.00	55.00	20.00	20.00	20.00	0.53	11.50	11.50	11.50	2.00
III	*m*	50.00	65.00	8.00	8.00	8.00	0.73	7.50	7.50	7.50	1.85
	n	70.00	75.00	14.00	14.00	14.00	1.11	9.00	9.00	9.00	2.10

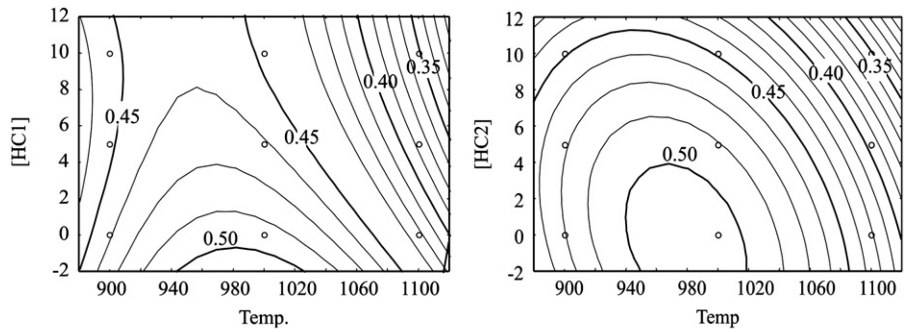

Fig. 2. Objective function for group I products.

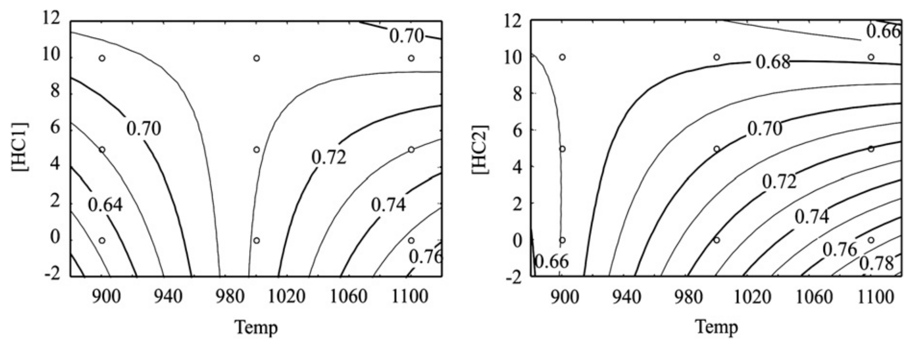

Fig. 3. Objective function for group II products.

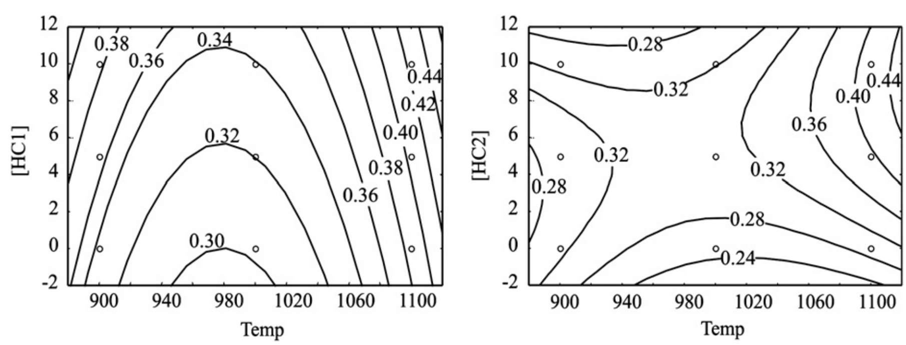

Fig. 4. Objective function for group III products.

the same influence on the function F

$$F(\text{Temp},[\text{HC1}],[\text{HC2}]) = \frac{\overline{CSB}+\overline{CSC}}{4} + \frac{\overline{WAT}+\overline{WAB}+\overline{WAC}}{6} + \frac{\overline{WLFT}+\overline{WLFB}+\overline{WLFC}}{6} + \frac{\overline{FS}}{2} + \frac{\overline{VMC}}{2} \quad (4)$$

The maximum of function F represents the optimal parameters for processing parameters, and also the optimum *CSB*, *CSC*, *WAT*, *WAB*, *WAC*, *FS*, *WLFT*, *WLFB*, *WLFC* or *VMC*. The graphs of the dependent variables with significant parameters were obtained using objective function to determine optimum production conditions, plotted on optimization graphic. If the value of membership trapezoidal function is close to 1, it shows the tendency of tested processing parameters of being optimal. Values of m and n for *CSB*, *CSC*, *WAT*, *WAB* and *WAC* were published in our previous research [10], but were even refined in this analysis.

According to Table 7, our samples belong to Group II, which is confirmed by optimization. Although the samples are of a loess nature, they contained buried soil and it marked them useful for hollow blocks production. Optimization process parameters for Group I were as follows: firing temperature of 980 °C, concentration of HC1 in the range of 0–2% and concentration of HC2 from 4–6%. Optimizing function F gained 0.52 value. The same parameters obtained for Group II were 980 °C, 0–5% and 8–10%, respectively, with 0.79 for optimizing function F. Process parameters gained for group III were: firing temperature of 1050 °C, HC1 concentration 8–10%, and HC2 concentration 10%, with 0.42 F function value.

The objective functions, regarding processing parameters, temperature and concentrations of added heavy clays were shown on the surface plots, for Groups I, II and III (Figs. 2, 3 and 4).

To determine the adequacy of the models, independent experiments were performed at optimum conditions for validation. Table 8 shows the model validation results. It was proved that the predicted values were comparable to the actual values in the experiment. Very good coefficients of variation (CV), which is less than 10% for all process variables, were calculated. CV values, higher than 15% for response variables, showed great influence to the statistically minor significance of its SOP model. The low CV values for response variables *CSB*, *CSC*, *WAT*, *WAB*, *WAC*, *FS*, *WLFT*, *WLFB*, *WLFC* or *VMC* indicated the adequacy of these models.

4. Conclusions

In this research, three heavy clays from the near locations are used. Representative clay, containing about 28% of clay sized particles was enriched with combined addition of two samples having about 42% and 40% of finest particles. Since the samples were of the loess nature, they contained high content of calcite and a lower content of dolomite. Experimental design and response surface analysis revealed that the sample containing more clay sized particles and less carbonates influenced better improvement of the final product. All the analyzed responses (compressive strength, water absorption, firing shrinkage, weight loss during firing and apparent density)

Table 8
Predicted and observed response variables at optimum conditions.

	Parameters	Predicted	Observed	Standard deviation	Coeff. of variation
Group I	*CSB*	25.70	25.78	1.90	7.39
	CSC	40.11	39.72	1.17	2.92
	WAT	19.00	18.88	0.26	1.37
	WAB	18.12	18.07	1.26	6.93
	WAC	13.58	13.65	0.69	5.08
	FS	1.19	1.20	0.01	0.86
	WLFT	9.47	9.49	0.26	2.75
	WLFB	9.82	9.89	0.37	3.76
	WLFC	10.26	10.32	0.31	2.99
	VMC	1.75	1.76	0.09	5.21
Group II	*CSB*	38.46	38.16	2.30	5.98
	CSC	54.13	54.50	2.71	5.00
	WAT	16.91	17.00	0.93	5.48
	WAB	16.23	16.20	1.23	7.59
	WAC	9.81	9.87	0.03	0.32
	FS	0.56	0.56	0.01	2.42
	WLFT	9.92	9.99	0.54	5.42
	WLFB	10.37	10.35	0.54	5.21
	WLFC	10.89	10.92	0.30	2.74
	VMC	1.78	1.77	0.13	7.43
Group III	*CSB*	37.43	37.21	2.40	6.42
	CSC	62.17	61.76	1.24	1.99
	WAT	17.67	17.57	1.18	6.68
	WAB	17.16	17.23	0.05	0.32
	WAC	10.73	10.72	0.88	8.22
	FS	1.07	1.07	0.03	3.05
	WLFT	9.63	9.70	0.46	4.82
	WLFB	10.18	10.24	0.15	1.47
	WLFC	10.68	10.68	0.03	0.28
	VMC	1.78	1.78	0.11	6.05

showed significant correlations among each other. Principal component analysis and analysis of variance showed that parameter most influencing responses were linear term of temperature. After fuzzy synthetic optimization, it was concluded that the most optimal combination of independent variables (firing temperature and concentration of added heavy clays) were temperature of 980 °C, [HC1] from 0 to 5% and [HC2] from 8 to 10%, and that these raw materials should be used in production of hollow blocks. The obtained conclusions are planned to be checked by industrial probes.

Acknowledgments

The authors are grateful to Serbian Ministry of Science and Technological Development for the financial support of this investigation included in the projects III450080 and TR 31055, project cycle 2011–2014.

References

[1] B. Strazzera, M. Dondi, M. Marsigli, Composition and ceramic properties of tertiary clays from southern Sardinia (Italy), Applied Clay Science 12 (3) (1997) 247–266.
[2] M. Dondi, Clay materials for ceramic tiles from the Sassuolo District (Northern Apennines, Italy). Geology, composition and technological properties, Applied Clay Science 15 (3–4) (1999) 337–366.
[3] H.G.F. Winkler, Bedeutung der Korngrössen-verteilung und Mineral-bestandes von tonnen für die Herstellung grobkeramischer Erzeugnisse, Berichte der DKG (1954) 31 667–343.
[4] H. Baccour, M. Medhioub, F. Jamoussic, T. Mhiri, Influence of firing temperature on the ceramic properties of Triassic clays from Tunisia, Journal of Materials Processing Technology 209 (2009) 2812–2817.
[5] M. Romero, A. Andrés, R. Alonso, J. Viguri, J. Ma, Rincón, Sintering behaviour of ceramic bodies from contaminated marine sediments, Ceramics International 34 (8) (2008) 1917–1924.
[6] J. García-Ten, M.J. Orts, A. Saburit, G. Silva, Thermal coductivity of traditional ceramics. Part I: influence of bulk density and firing temperature, Ceramics International 36 (2010) 1951–1959.
[7] L.C.S. Herek, C.E. Hori, M.H.M. Reis, N.D. Mora, C.R.G. Tavares, R. Bergamasco, Characterization of ceramic bricks incorporated with textile laundry sludge, Ceramics International 38 (2012) 951–959.
[8] C. Manoharan, P. Sutharsan, S. Dhanapandian, R. Venkatachalapathy, R.M. Asanulla, Analysis of temperature effect on ceramic brick production from alluvial deposits, Tamilnadu, India, Applied Clay Science 54 (2011) 20–25.
[9] M. Arsenović Z. Radojević S. Stanković Ž. Lalić L. Pezo, What to expect from heavy clay?, Ceramics International http://dx.doi.org/10.1016/j.ceramint.2012.08.009, in press.
[10] M. Arsenović, S. Stanković, Z. Radojević L. Pezo, Prediction and fuzzy synthetic optimization of process parameters in heavy clay brick production http://dx.doi.org/10.1016/j.ceramint.2012.08.053, in press.
[11] S.L. Correia, D. Hotza, A.M. Segadães, Simultaneous optimization of linear firing shrinkage and water absorption of triaxial ceramic bodies using experiments design, Ceramics International 30 (2004) 917–922.
[12] D. Njoya, M. Hajjaji, D. Njopwouo, Effects of some processing factors on technical properties of a clay-based ceramic material, Applied Clay Science 65–66 (2012) 106–113.
[13] J. Li, J. Peng, S. Guo, L. Zhang, Application of response surface methodology (RSM) for optimization of sintering process for the preparation of magnesia partially stabilized zirconia (Mg-PSZ) using natural baddeleyite as starting material, Ceramics International http://dx.doi.org/10.1016/j.ceramint.2012.06.009, in press.
[14] Z. Radojević, Z. Lalić, R. Vasić, A. Mitrović, Brick raw materials quality in Serbia and the influence for the products quality and to the production technology—loess sediments, Izgradnja 59 (2005) 45–49.
[15] S.B. Marković, N.S. Kostić, E.A. Oches, Paleosols in the Ruma loess section (Vojvodina, Serbia), Revisita Mexicana de Ciencias Geológicas 21 (2004) 79–87.
[16] I.J. Smalley, I.F. Jefferson, T.A. Dijkstra, E. Derbyshire, Some major events in the development of the scientific study of loess, Earth-Science Reviwes 54 (2001) 5–18.
[17] Project report: Revision of Regional Waste Management Plan for the City of Zrenjanin and Municipalities Sečanj, Titel and Kovačica, University of Novi Sad, Faculty of Technical Sciences. Available online from: 〈http://www.zrenjanin.rs/userfiles/file/Zastita%20zivotne%20sredine/2011/upravljanje%20odpadom/RPUOZRENJANINSECANJTITELKOVACICA.pdf〉, 2011 (accessed 10.09.2012), (in Serbian).
[18] D.M. Moore, R.C. Reynolds Jr., Sample preparation techniques for clay minerals. Preparing the oriented clay mineral aggregate. In: X-ray Diffraction and the Identification and Analysis of Clay Minerals, Oxford University Press, USA, 1997, p. 214 (Chapter 6).
[19] M.M. Jordan, A. Boix, T. Sanfeliu, C. De la Fuente, Firing transformations of cretaceous clays used in the manufacturing of ceramic tiles, Applied Clay Science 14 (1999) 225–234.
[20] C.M.F. Veira, R. Sanchez, S.N. Monteiro, Characteristics of clays and properties of building ceramics in the state of Rio de Janeiro, Brazil, Construction and Building Materials 22 (2008) 781–787.
[21] SRPS EN 771-1, Specification for masonry units—Part 1: Clay masonry units, 2010.
[22] 〈http://www.bsieducation.org/Education/downloads/tests/02density.pdf〉.
[23] G.E.P. Box, D.W. Behnken, Some new three level designs for the study of quantitative variables, Technometrics 2 (1960) 455–475.
[24] S. Meseguer, T. Sanfeliu, M.M. Jordan, Classification and statistical analysis of mine spoils chemical composition from Oliete basin (Teruel, NE Spain), Environmental Geology 56 (2009) 1461–1466.
[25] R.J. Merriman, D.E. Highley, D.G. Cameron, Definition and characteristics of very-fine grained sedimentary rocks: clay, mudstone, shale and slate. British geological Survey Commissioned Report CR/03/281N, 1999.
[26] J García-Ten, M.J. Orts, A. Saburit, G. Silva, Thermal coductivity of traditional ceramics. Part II: influence of mineralogical composition, Ceramics International 36 (2010) 2017–2024.
[27] E. Furlani, G. Tonello, E. Aneggi, S. Maschio, Preparation and characterization of sintered ceramics made with spent foundry olivine sand and clay, Ceramics International 38 (2012) 2619–2625.